LAWRENCE
LIVERMORE
NATIONAL
LABORATORY

LLNL-JRNL-613272

A Simple Solution to the Fresnel-Kirchoff Diffraction Integral for Application to Refraction-Enhanced Radiography

J. A. Koch, O. L. Landen, L. J. Suter, L. P. Masse

January 25, 2013

Journal of the Optical Society of America A

A Simple Solution to the Fresnel-Kirchoff Diffraction Integral for Application to Refraction-Enhanced Radiography

J. A. Koch,[1,*] O. L. Landen,[1] L. J. Suter,[1] L. P. Masse[2]

[1]Lawrence Livermore National Laboratory, P. O. Box 808, L-493, Livermore, CA, 94550
[2]CEA, DAM, DIF, F-91297 Arpajon, France
**Corresponding author: koch1@llnl.gov*

Received Month X, XXXX; revised Month X, XXXX; accepted Month X, XXXX; posted Month X, XXXX (Doc. ID XXXXX); published Month X, XXXX

We present a simple solution to the one-dimensional Fresnel-Kirchoff diffraction integral with minimal approximations that are appropriate for the geometrical optics regime, where phase contrast enhancements can be considered to be caused by refraction by a semi-transparent object. We demonstrate its accuracy by comparison to brute-force numerical raytrace and diffraction calculations of a representative simulated object, and show excellent agreement for spatial scales corresponding to Fresnel numbers greater than unity. The result represents a significant improvement over approximate formulas typically used in analysis of refraction-enhanced radiographs, particularly for radiography of transient phenomena in objects that strongly refract and show significant absorption.

OCIS Codes: 340.7440, 050.1960, 110.1650, 110.2990

Backlit projection x-ray radiography of absorbing objects has a long history dating back to Röntgen. In the limit of high x-ray energy, transmission of backlight x-rays along a line of sight is $e^{-\tau}$, where τ is the line-integrated opacity of the object that depends on the object material properties and the backlight x-ray energy. Treating τ as one-dimensional is a natural simplification for imaging spherically-symmetric objects, in which case $\tau(x)$ is the Abel transform of a radial attenuation coefficient. This class of objects is important for radiography of inertial-confinement fusion (ICF) plasmas [1-3].

This approach fails when wave effects becomes significant. From a diffraction perspective, a light wave from a backlight source experiences a local phase shift $\phi(x)$ relative to vacuum in passing through a semi-transparent object, and over sufficient propagation distances the phase perturbations generate light intensity perturbations in a detector plane. From a geometrical optics perspective, straight rays from the backlight source are refracted by transverse density gradients in the object, and this adds or subtracts light intensity locally in a detector plane. The two perspectives are equivalent for object spatial scales L, propagation distances q, and light wavelengths λ that correspond to Fresnel numbers $F = L^2/q\lambda >> 1$. This refraction-enhanced imaging regime is of interest in fields such as biological and medical imaging and astronomy [4-9], and is of greatest interest for ICF research [10].

The transport of intensity equation (TIE) [11-13] is typically used to interpret the transmitted intensity pattern I(x,z) along the z-axis line of sight,

$$\frac{\partial I}{\partial z} = \frac{-\lambda}{2\pi}\left(I\frac{d^2\phi}{dx^2} + \frac{\partial I}{\partial x}\frac{d\phi}{dx}\right) \quad (1)$$

Direct application of eq. (1) is limited to small offsets and/or multiple detector planes. When absorption is negligible and phase shifts are small, the intensity $I(x,q) = 1 - (\lambda q/2\pi)d^2\phi(x,0)/dx^2$ [4,14,15], and modifications to allow for absorption can also be included [16-18]. Retrieval of $\phi(x)$ can then proceed using a variety of approaches. An alternative approach is to map deflections by scanning across the object [5,14], and this provides a direct measure of $d\phi/dx$ when the approach is practical.

Transient phenomena in strongly refracting and absorbing objects present a particular problem, because scanning or detector-plane shifting techniques cannot be used, and $\phi(x)$ and $\tau(x)$ must generally be found iteratively using model functions in a forward fit. Approximate formulas used for calculating I(x) fail because the required approximations do not hold, and in this case numerical forward calculations of I(x) using either eq. (1) , numerical raytracing, or direct solution of the Fresnel-Kirchoff (FK) integral [19,20] must be used. This process is time-consuming, particularly when model functions are developed without assumed analytic forms in genetic algorithm search and reconstruction procedures [21]. We therefore pursue the derivation of a simple formula for the radiograph intensity distribution due to a strongly refracting and absorbing object in an arbitrary detector plane that is appropriate for the refraction-enhanced imaging regime.

We begin with the one-dimensional complex form of the FK diffraction integral for an infinitely-distant source backlighting an absorbing phase object in vacuum, with phase and opacity variations along the x-axis immediately in front of the object, and look for solutions to the free-space propagation problem that leads to an absorption radiograph with refractive enhancements. The field at location x in a detector plane a distance q behind the object can be written as,

$$E(x) = C\int_{-\infty}^{\infty}\left(\frac{1}{2} + \frac{1}{2\sqrt{1+(x-x_o)^2/q^2}}\right) e^{\frac{-\tau(x_o)}{2}} e^{i\left(\frac{2\pi q}{\lambda}\sqrt{1+\frac{(x-x_o)^2}{q^2}}+\phi(x_o)-\frac{\pi}{2}\right)} dx_o \quad (2)$$

where C is a normalization constant and x_o is the coordinate in the object plane. We assume $(x - x_o)^2 << q^2$

and $\lambda \ll q$, eliminating the slowly-varying bracketed obliquity factor and simplifying the phase exponential. When $\phi(x_o)$ = constant and $\tau(x_o) = 0$, we can solve the integral analytically [22] and determine C such that the intensity $I(x) = |E(x)E^*(x)|$ is unity. Neglecting phase factors that will cancel in I(x) throughout, we have,

$$E(x) = \frac{1}{\sqrt{\lambda q}} \int_{-\infty}^{\infty} e^{\frac{-\tau(x_o)}{2}} e^{i\left(\phi(x_o) + \frac{\pi(x-x_o)^2}{\lambda q}\right)} dx_o \tag{3}$$

We now work with eq. (3) directly in coordinate space, rather than with transforms in Fourier space. We change variables with $u = (x - x_o)/a$, yielding

$$E(x) = \frac{1}{\sqrt{\pi}} \int_{-\infty}^{\infty} e^{\frac{-\tau(x-au)}{2}} e^{i\left(\phi(x-au) + u^2\right)} du \tag{4}$$

with $a = \sqrt{\lambda q/\pi}$. We first expand ϕ about x, setting derivatives higher than $\phi_2 = d^2\phi/dx^2$ equal to zero,

$$E(x_d) = \frac{1}{\sqrt{\pi}} \int_{-\infty}^{\infty} e^{\frac{-\tau(x_d-au)}{2}} e^{i\left(\phi(x_d) - au\phi_1(x_d) + (1+\frac{a^2\phi_2(x_d)}{2})u^2\right)} du \tag{5}$$

Eq. (5) can be rewritten as,

$$\begin{aligned} E(x) &= \frac{1}{\sqrt{\pi}} \int_{-\infty}^{\infty} e^{\frac{-\tau(x-au)}{2}} e^{i\left(\left(1+\frac{a^2\phi_2(x)}{2}\right)u^2 - au\phi_1(x)\right)} du \\ &= \frac{1}{\sqrt{\lambda q}} \int_{-\infty}^{\infty} e^{\frac{-\tau(x_o)}{2}} e^{i\left(\sqrt{1+\frac{a^2\phi_2(x)}{2}}\frac{(x-x_o)}{a} - \frac{a\phi_1(x)}{2\sqrt{1+\frac{a^2\phi_2(x)}{2}}}\right)^2} dx_o \end{aligned} \tag{6}$$

We recognize that eq. (6) implies that object points near $x_o = x$ contribute most to the field (u near zero) at a detector location x' that is different from x, and that the intensity pattern will therefore be shifted locally by an amount that eliminates the second term in the exponential. We find the shift by writing E(x'), with $x' = x + a^2\phi_1(x)/2$. Again neglecting third- and higher-order derivatives of $\phi(x)$, this is,

$$\begin{aligned} E(x') = E(x + \frac{a^2\phi_1(x)}{2}) &= \frac{1}{\sqrt{\lambda q}} \int_{-\infty}^{\infty} e^{\frac{-\tau(x_o)}{2}} e^{i\left(1+\frac{a^2}{2}\phi_2(x)\right)\left(\frac{(x-x_o)}{a}\right)^2} dx_o \\ &= \frac{1}{\sqrt{1+\frac{a^2}{2}\phi_2(x)}} \frac{1}{\sqrt{\pi}} \int_{-\infty}^{\infty} e^{\frac{-\tau(x-bu)}{2}} e^{iu^2} du \end{aligned} \tag{7}$$

where $b^2 = a^2/(1 + a^2\phi_2(x)/2)$. We next expand $\tau(x)$ about x and set derivatives higher than $\tau_2 = d^2\tau/dx^2$ equal to zero, giving,

$$E(x') = \frac{b e^{\frac{-\tau(x)}{2}}}{\sqrt{\lambda q}} \int_{-\infty}^{\infty} e^{-\left(\frac{b^2\tau_2}{4}u^2 - \frac{b\tau_1}{2}u\right)} e^{-iu^2} du \tag{8}$$

The integral can be solved analytically [22], and the resulting intensity is,

$$\begin{aligned} I(x') &= I(x + \frac{\lambda q\phi_1}{2\pi}) = \frac{e^{-\tau}}{\left|1 + \frac{\lambda q\phi_2}{2\pi}\right|} K(x) \\ K(x) &= \frac{e^{\frac{\lambda^2 q^2}{32\pi^2}\frac{\tau_1^2\tau_2}{\left(\left(1+\frac{\lambda q\phi_2}{2\pi}\right)^2 + \frac{\lambda^2 q^2\tau_2^2}{16\pi^2}\right)}}}{\sqrt{1 + \frac{\lambda^2 q^2 \tau_2^2}{16\pi^2\left(1+\frac{\lambda q\phi_2}{2\pi}\right)^2}}} \approx 1 + \frac{1}{8}\left(\frac{\lambda q}{2\pi}\right)^2 \frac{\tau_2(\tau_1^2 - \tau_2)}{\left(1+\frac{\lambda q\phi_2}{2\pi}\right)^2} \end{aligned} \tag{9}$$

where τ and all derivatives are evaluated at x. Eq. (9) is an exact solution for the intensity pattern derived from fields given by the FK integral of eq. (3), assuming only that terms involving third- and higher-order derivatives in the expansions of $\phi(x+\delta)$ and $\tau(x+\delta)$ about x are all zero. From eq. (4), it is therefore well-suited to the geometrical optics regime of Fresnel numbers much larger than unity.

The term K(x) is second-order in λq and involves squares of first and second derivatives of the opacity profile, and in most cases of practical interest can be neglected. Eq. (9) then reduces to a particularly simple form,

$$I(x + \frac{\lambda q}{2\pi}\frac{d\phi(x)}{dx}) = \frac{e^{-\tau(x)}}{\left|1 + \frac{\lambda q}{2\pi}\frac{d^2\phi(x)}{dx^2}\right|} \tag{10}$$

Eq. (10) differs in three important respects from approximate equations used to describe intensity patterns in refraction-enhanced imaging [13-20]; the intensity pattern is shifted on the left-hand side by an amount proportional to $d\phi/dx$, the right-hand side involves $1/|1 + (\lambda q/2\pi)d^2\phi/dx^2|$ rather than $1 - (\lambda q/2\pi)d^2\phi/dx^2$, and absorption is included by simply multiplying the right-hand side by an exponential absorption factor. Where the second derivative term in the denominator of the right-hand side is less than negative one, a cusp is formed and the intensity profile forms caustics. In these regions the intensities of the folds simply add, though here the neglect of third- and higher-order derivatives of $\phi(x)$ and $\tau(x)$ in this treatment may become questionable.

Approximate solutions for I(x), rather than I(x'), can be attempted, and the first approximation for infinitesimal q recovers the TIE eq. (1), but eq. (10) is perhaps most useful as-written for forward-fit iterative solutions to the inversion problem of determining $\phi(x)$ and $\tau(x)$ from intensity radiograph data. Given trial functions $\phi(x)$ and $\tau(x)$, the intensity pattern can be easily calculated with minimal restrictions on their higher-order derivatives, allowing rapid iteration to optimal $\phi(x)$ and $\tau(x)$ functions by generating regridded radiographs I(x') that best match experimental data. The equation is equally appropriate for point-source projection radiography when x is the detector location scaled back to the object through the magnification and when q is replaced by $f = pq/(p+q)$, where p is the source/object distance [10,15,16].

We can demonstrate the accuracy of eq. (10) using simulations appropriate to radiography of an ICF implosion [10]. Fig. 1(a) shows typical expected radial electron density and absorption coefficient (at E = 10 keV) profiles along with their corresponding line-integrated $\phi(x)$ and $\tau(x)$ profiles that are the Abel transforms of the radial profiles. We see that this object is strongly refracting and absorbing when viewed along the limb, with ~ 300 radians of phase shift, peak optical depths > 1, and spatial scales down to ~ 1 μm. Fig. 1(b) shows a comparison of expected radiograph profiles from a 10 keV collimated x-ray source backlighting the implosion onto a detector q = 10 mm from the object (equivalent to point-source backlighting at high magnification, with p = 10 mm), calculated in various ways; numerical raytracing [10,23], direct application of the FK integral eq. (2), eq. (10), and

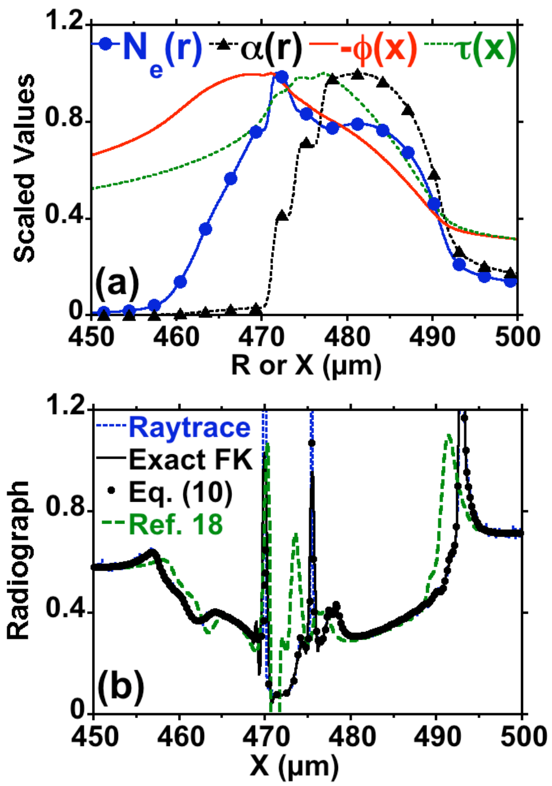

Fig 1: (a) Radial electron density $N_e(r)/2.6\text{x}10^{24}$ cm^{-3}, radial absorption coefficient $\alpha(r)/3.9\text{x}10^{-3}$ μm^{-1}, phase shift $-\phi(x)/285$ radians, and opacity $\tau(x)/1.12$, and (b) simulated radiographs described in the text.

eq. (33) of [18] that derives from [17] for infinite source distance. We see that eq. (10) duplicates a numerical raytrace even in the sharply-varying caustic region near x = 470 μm, and duplicates direct application of the FK integral except where $\phi(x)$ significantly varies over μm spatial scales corresponding to Fresnel numbers < 1, where the higher-order derivatives neglected in the derivation of eq. (10) are significant. It also significantly improves upon previous approximate formulas, which misplace the peaks and dips and calculate negative intensities near x = 470 μm.

In summary, we have derived and demonstrated a simple analytical formula to predict the radiograph profile of an arbitrary absorbing and phase-shifting object, that is an exact solution to the Fresnel-Kirchoff integral with well-specified approximations appropriate to the refraction-enhanced imaging regime. This represents a significant improvement over earlier approximate formulas for radiography of transient phenomena in objects that are strongly refracting and absorbing, and is well-suited to iterative search and reconstruction procedures that optimize the phase and opacity profiles to best-fit individual measured radiographs. This work was performed under the auspices of the U.S. Department of Energy by Lawrence Livermore National Laboratory under contract DE-AC52-07NA27344.

References

1. D. H. Kalantar, S. W. Haan, B. A. Hammel, C. J. Keane, O. L. Landen, D. H. Munro, Rev. Sci. Instrum. **68**, 814 (1997).
2. F. J. Marshall, P. W. McKenty, J. A. Delettrez, R. Epstein, J. P. Knauer, V. A. Smalyuk, J. A. Frenje, C. K. Li, R. D. Petrasso, F. H. Sequin, R. C. Mancini, Phys. Rev. Lett. **102**, 185004 (2009).
3. D. G. Hicks, B. K. Spears, D. G. Braun, R. E. Olson, C. M. Source, P. M. Celliers, G. W. Collins, O. L. Landen, Phys. Plasmas **17**, 102703 (2010).
4. S. W. Wilkins, T. E. Gureyev, D. Gao, A. Pogany, A. W. Stevenson, Nature **384**, 335 (1996).
5. D. Chapman, W. Thomlinson, R. E. Johnson, D. Washburn, E. Pisano, N. Gmür, Z. Zhong, R. Menk, F. Arfelli, D. Sayers, Phys. Med. Biol. **42**, 2015 (1997).
6. N. Yagi, Y. Suzuki, K. Umetani, Y. Kohmura, K. Yamasaki, Med. Phys. **26**, 2190 (1999).
7. J. Keyriläinen, M. Fernández, P. Suortti, Nuc. Instrum. Meth. Phys. Res. A **488**, 419 (2002).
8. M. N. Wernick, Y. Yang, I. Mondal, D. Chapman, M. Hasnah, C. Parham, E. Pisano, Z. Zhong, Phys. Med. Biol. **51**, 1769 (2006).
9. A. Clegg, A. L. Fey, T. J. W. Lazio, Astrophys. J. **496**, 253 (1998).
10. J. A. Koch, O. L. Landen, B. J. Kozioziemski, N. Izumi, E. L. Dewald, J. D. Salmonson, B. A. Hammel, J. Appl. Phys. **105**, 113112 (2009).
11. K. A. Nugent, T. E. Gureyev, D. F. Cookson, D. Paganin, Z. Barnea, Phys. Rev. Lett. **77**, 2961 (1996).
12. T. E. Gureyev, C. Raven, A. Snigirev, I. Snigireva, S. W. Wilkins, J. Phys. D. **32**, 563 (1999).
13. K. Nugent, J. Opt. Soc. Am. A **24**, 536 (2007).
14. Y. Suzuki, N. Yagi, K. Uesugi, J. Synch. Rad. **9**, 160 (2002).
15. A. Pogany, D. Gao, S. W. Wilkins, Rev. Sci. Instrum. **68**, 2774 (1997).
16. T. E. Gureyev, S. W. Wilkins, J. Opt. Soc. Am. A **15**, 579 (1998).
17. T. E. Gureyev, S. Mayo, S. W. Wilkins, D. Paganin, A. W. Stevenson, Phys. Rev. Lett. **86**, 5827 (2001).
18. X. Wu, H. Liu, J. X-ray Sci. Tech. **11**, 33 (2003).
19. E. Hecht, A. Zajac, *Optics* (Addison-Wesley, Reading, 1974).
20. M. Born, E. Wolf, *Principles of Optics*, 2nd Ed. (Pergamon, New York, 1964).
21. I. Golovkin, R. Mancini, S. Louis, Y. Ochi, K. Fujita, H. Nishimura, H. Shirga, N. Miyanaga, H. Azechi, R. Butzback, I. Uschmann, E. Förster, J. Delettrez, J. Koch, R. W. Lee, L. Klein, Phys. Rev. Lett. **88**, 045002 (2002)
22. I. Gradshteyn, I. Ryzhik, *Table of Integrals, Series, and Products*, 7th Ed. (Elsevier, Amsterdam, 2007).
23. J. A. Koch, J. D. Sater, A. J. MacKinnon, T. P. Bernat, D. N. Bittner, G. W. Collins, B. A. Hammel, E. R. Mapoles, C. H. Still, Fusion Sci. and Tech. **43**, 55 (2003).

Full References (Page 4)

1. D. H. Kalantar, S. W. Haan, B. A. Hammel, C. J. Keane, O. L. Landen, and D. H. Munro, "X-ray backlit imaging measurement of in-flight pusher density for an indirect drive capsule implosion", Rev. Sci. Instrum. **68**, 814-816 (1997).
2. F. J. Marshall, P. W. McKenty, J. A. Delettrez, R. Epstein, J. P. Knauer, V. A. Smalyuk, J. A. Frenje, C. K. Li, R. D. Petrasso, F. H. Sequin, and R. C. Mancini, "Plasma-density determination from x-ray radiography of laser-driven spherical implosions", Phys. Rev. Lett. **102**, 185004 (2009).
3. D. G. Hicks, B. K. Spears, D. G. Braun, R. E. Olson, C. M. Source, P. M. Celliers, G. W. Collins, and O. L. Landen, "Convergent ablator performance measurements", Phys. Plasmas **17**, 102703 (2010).
4. S. W. Wilkins, T. E. Gureyev, D. Gao, A. Pogany, and A. W. Stevenson, "Phase contrast imaging using polychromatic hard x-rays", Nature **384**, 335-338 (1996).
5. D. Chapman, W. Thomlinson, R. E. Johnson, D. Washburn, E. Pisano, N. Gmür, Z. Zhong, R. Menk, F. Arfelli, and D. Sayers, "Diffraction enhanced x-ray imaging", Phys. Med. Biol. **42**, 2015-2025 (1997).
6. N. Yagi, Y. Suzuki, K. Umetani, Y. Kohmura, and K. Yamasaki, "Refraction-enhanced x-ray imaging of mouse lung using synchrotron radiation source", Med. Phys. **26**, 2190-2193 (1999).
7. J. Keyriläinen, M. Fernández, and P. Suortti, "Refraction contrast in x-ray imaging", Nuc. Instrum. Meth. Phys. Res. A **488**, 419-427 (2002).
8. M. N. Wernick, Y. Yang, I. Mondal, D. Chapman, M. Hasnah, C. Parham, E. Pisano, and Z. Zhong, "Computation of mass-density images from x-ray refraction-angle images", Phys. Med. Biol. **51**, 1769-1778 (2006).
9. A. Clegg, A. L. Fey, and T. J. W. Lazio, "The gaussian plasma lens in astrophysics: Refraction", Astrophys. J. **496**, 253-266 (1998).
10. J. A. Koch, O. L. Landen, B. J. Kozioziemski, N. Izumi, E. L. Dewald, J. D. Salmonson, and B. A. Hammel, "Refraction-enhanced x-ray radiography for inertial confinement fusion and laser-produced plasma applications", J. Appl. Phys. **105**, 113112 (2009).
11. K. A. Nugent, T. E. Gureyev, D. F. Cookson, D. Paganin, and Z. Barnea, "Quantitative phase imaging using hard x-rays", Phys. Rev. Lett. **77**, 2961-2964 (1996).
12. T. E. Gureyev, C. Raven, A. Snigirev, I. Snigireva, and S. W. Wilkins, "Hard x-ray quantitative non-interferometric phase-contrast microscopy", J. Phys. D. **32**, 563-567 (1999).
13. K. Nugent, "X-ray noninterferometric phase imaging: A unified picture", J. Opt. Soc. Am. A **24**, 536-547 (2007).
14. Y. Suzuki, N. Yagi, and K. Uesugi, "X-ray refraction-enhanced imaging and a method for phase retrieval for a simple object", J. Synch. Rad. **9**, 160-165 (2002).
15. A. Pogany, D. Gao, and S. W. Wilkins, "Contrast and resolution in imaging with a microfocus x-ray source", Rev. Sci. Instrum. **68**, 2774-2782 (1997).
16. T. E. Gureyev and S. W. Wilkins, "On x-ray phase imaging with a point source", J. Opt. Soc. Am. A **15**, 579-585 (1998).
17. T. E. Gureyev, S. Mayo, S. W. Wilkins, D. Paganin, and A. W. Stevenson, "Quantitative in-line phase contrast imaging with multienergy x-rays", Phys. Rev. Lett. **86**, 5827-5830 (2001).
18. X. Wu and H. Liu, "A general theoretical formalism for x-ray phase contrast imaging", J. X-ray Sci. Tech. **11**, 33-42 (2003).
19. E. Hecht and A. Zajac, *Optics* (Addison-Wesley, Reading, 1974).
20. M. Born and E. Wolf, *Principles of Optics*, 2nd Ed. (Pergamon, New York, 1964).
21. I. Golovkin, R. Mancini, S. Louis, Y. Ochi, K. Fujita, H. Nishimura, H. Shirga, N. Miyanaga, H. Azechi, R. Butzback, I. Uschmann, E. Förster, J. Delettrez, J. Koch, R. W. Lee, and L. Klein, "Spectroscopic determination of dynamic plasma gradients in implosion cores", Phys. Rev. Lett. **88**, 045002 (2002)
22. I. Gradshteyn and I. Ryzhik, *Table of Integrals, Series, and Products*, 7th Ed. (Elsevier, Amsterdam, 2007).
23. J. A. Koch, J. D. Sater, A. J. MacKinnon, T. P. Bernat, D. N. Bittner, G. W. Collins, B. A. Hammel, E. R. Mapoles, and C. H. Still, "Numerical raytrace verification of optical diagnostics of ice surface roughness for inertial confinement fusion experiments", Fusion Sci. and Tech. **43**, 55-66 (2003).